Multiscaling Properties of Large-Scale Structure in the Universe

V. J. Martínez, S. Paredes, S. Borgani, P. Coles

The large-scale distribution of galaxies and galaxy clusters in the universe can be described in the mathematical language of multifractal sets. A particularly significant aspect of this description is that it furnishes a natural explanation for the observed differences in clustering properties of objects of different density in terms of multiscaling, the generic consequence of the application of a local density threshold to a multifractal set. The multiscaling hypothesis suggests ways of improving upon the traditional statistical measures of clustering pattern (correlation functions) and exploring further the connection between clustering pattern and dynamics.

One of the key problems in modern cosmology is understanding how the spatial clustering of objects such as galaxies and galaxy clusters can provide clues about the evolution of primordial density inhomogeneities under the action of gravitational instability. The traditional tool for quantifying the spatial correlations of cosmological objects is the two-point correlation function $\xi(r)$, defined in terms of the probability δP of finding a pointlike object of a given type, such as a galaxy, in a small volume δV at a distance r from a given object of the same type

$$\delta P = n[1 + \xi(r)]\delta V \qquad (1)$$

where n is the mean number density of objects. The two-point correlation function for galaxies, $\xi_{gg}(r)$, is well fitted by a power law in the range $r = 0.1h^{-1}$ to $10h^{-1}$ Mpc (*1, 2*): $\xi_{gg}(r) = (r/r_0)^{-\gamma}$, with an exponent $\gamma \approx 1.8 \pm 0.1$ and a correlation length $r_0 \approx (5 \pm 1)h^{-1}$ Mpc (h is the Hubble constant in units of 100 km s^{-1} Mpc^{-1}). Analyses of samples of galaxy clusters, however, have yielded power-law fits to the cluster-cluster correlation function, $\xi_{cc}(r)$, of a form similar to that of $\xi_{gg}(r)$ but with exponents (*3–10*) varying in the range $\gamma = 1.6$ to 2.6 and correlation lengths from $13h^{-1}$ to $30h^{-1}$ Mpc, with a strong dependence of r_0 on the richness class of the clusters selected (*11, 12*).

Szalay and Schramm (*13*) noted that the clustering correlation lengths $r_{0,i}$ for different classes of objects i can be described in terms of a unified scheme in which $r_{0,i}$ scales with mean separation: $r_{0,i} \propto d_i \equiv n_i^{-1/3}$, where n_i is the mean number density of the objects. If the two-point correlation functions of different classes of objects all have a power-law shape with almost the same exponent $\gamma \approx 1.8$, then $\xi(r)$ can be expressed in a universal dimensionless form (*14, 15*)

$$\xi_i(r) = \beta\left(\frac{r}{n_i^{-1/3}}\right)^{-\gamma} \qquad (2)$$

where $\beta = 0.2$ to 0.3 (*14, 15*). This relation is remarkably well fitted by optical clusters, x-ray clusters, groups of galaxies, quasi-stellar objects, and radio galaxies, and although there are still significant uncertainties in the power-law fits for clusters, the general trend of increasing r_0 with richness seems to be well established observationally and is reproduced in numerical simulations of cluster clustering (*16, 17*). On the other hand, optical galaxies and IRAS galaxies (those first observed with the Infrared Astronomical Satellite), the objects for which most data are available, do not appear to fit into this scheme (*14, 15, 18*), because they are characterized by larger values of $\beta \approx 1.1$ (*15*). This could be because small-scale ($<5h^{-1}$ Mpc) galaxy clustering is principally determined by nonlinear gravitational effects and is therefore enhanced with respect to the weakly nonlinear clustering displayed by clusters on large scales ($>20h^{-1}$ Mpc). In this report we shall show how these observational trends—in particular, the apparent difference in clustering behavior between clusters of galaxies and galaxies themselves—can be explained in terms of the multiscaling phenomenon, which is associated with the application of density thresholds to multifractal sets.

Scaling is said to occur in a geometrical pattern whenever some quantity describing the spatial distribution has a power-law dependence on scale. For example, fractal models of coastlines have a length L that depends on the resolution d used to measure it according to $L(d) \propto d^{1-D}$ for some non-integer D: in this case, D is the Hausdorff dimension of the coastline structure. In contrast to simple fractals like this, which are described by a single scaling dimension (D), multifractal sets involve a spectrum of scaling indices: the density around different points is characterized by different (local) fractal dimensions. A particularly important signature of multifractal scaling is the fact that moments of the distribution of differing order q scale in a manner described by different dimensions D_q (for a simple fractal, $D_q = D$ for all q). Such objects have proven extremely useful in describing a variety of nonlinear phenomena in turbulence, chaotic dynamics, and disordered systems (*19*), and there is now considerable evidence that galaxy clustering is intrinsically multifractal in character, perhaps connected with the supposed self-similarity of gravitational evolution (*20*).

In the context of galaxy clustering, the important exponent is the correlation dimension D_2, which is defined in terms of scaling of the correlation integral $C(r)$ over a distance s

$$C(r) = \int_0^r 4\pi n[1 + \xi(s)]s^2 ds = Ar^{D_2} \qquad (3)$$

where A is a constant. The index D_2 is a clean and easy to interpret measure of clustering strength: the larger the value of D_2, the weaker the large-scale clustering. Note that power-law scaling of $C(r)$ implies power-law scaling of $\xi(r)$ only if $\xi(r) \gg 1$. If this is the case, then Eq. 3 yields $D_2 \approx 3 - \gamma$. However, this equality is not expected to hold in the range of scales where the correlation function is of order unity. Consequently, if the correlation integral behaves as a power-law when $\xi(r) \sim 1$, the function $\xi(r)$ itself does not. By differentiating Eq. 3 with respect to r and putting $r = r_0$, we obtain

$$r_0 = \left(\frac{AD_2}{8\pi n}\right)^{1/(3-D_2)} \qquad (4)$$

which furnishes a useful estimator of r_0.

Multiscaling (*21*) is the general term given to scaling behavior in which the characteristic exponent (in this case D_2) is a slowly varying function of scale or of the threshold density used to select objects of different richness from an underlying distribution. This form of scaling is a general consequence of applying a density cutoff to a multifractal set. Regions of higher density in multifractal sets have smaller values of the scaling indices. If, for example, such a set is "censored" by removing all of the points where the local density is less than some given value ϵ, then the correlation dimension of the surviving set will be smaller than that of the uncensored set: $D_2(\epsilon) < D_2$.

V. J. Martínez, Departament d'Astronomia i Astrofísica, Universitat de València, Burjassot, 46100 València, Spain.
S. Paredes, Departament d'Astronomia i Astrofísica, Universitat de València, Burjassot, 46100 València, and Departamento de Matemáticas, Universidad de Murcia, Murcia, Spain.
S. Borgani, Istituto Nazionale di Fisica Nucleare–Sezione di Perugia, Dipartimento di Fisica, dell'Università, Via A. Pascoli, I-06100, Perugia, and Scuola Internazionale Superiore di Studi Avanzati (SISSA), Via Beirut 2-4, I-34014 Trieste, Italy.
P. Coles, Astronomy Unit, School of Mathematical Sciences, Queen Mary and Westfield College, Mile End Road, London E1 4NS, UK.

This kind of thresholding is reminiscent of the idea of "biasing" (*22*), in which regions of high primordial density are identified with observable objects. Our philosophy is, however, quite different from this in that we apply our thresholding to the nonlinear density field modeled as a multifractal, rather than the initial (Gaussian) density perturbations. In this respect, our approach improves considerably on the standard approach to biasing.

To demonstrate the applicability of this description to a realistic example, we first analyzed a series of numerical simulations of the distribution of rich clusters (*17*). In these simulations, clusters are identified as the highest peaks in the evolved density field. Consequently, cluster populations characterized by progressively larger mean separations d_i are selected by applying progressively higher density thresholds. A plane projection of the three-dimensional density field of one of these simulations is shown in Fig. 1 for a so-called CHDM model, in which 30% of the critical density of the universe is provided by one flavor of massive neutrinos and the remainder is made up mainly of cold relic particles (*23*). This model has been shown to be reasonably successful at accounting for observed large-scale structure. The morphology corresponds to that of a multifractal distribution, rather than a simple fractal. Figure 2 shows the correlation integral results for such simulated universes.

Table 1. Correlation length r_0 and correlation dimension D_2 at several values of the mean cluster separation d_i.

d_i (h^{-1} Mpc)	r_0 (h^{-1} Mpc)	D_2
20	6.5 ± 1.1	2.55 ± 0.02
30	15.5 ± 1.7	2.17 ± 0.03
40	19.7 ± 1.7	1.90 ± 0.03
50	22.3 ± 1.5	1.70 ± 0.03
60	24.0 ± 1.3	1.54 ± 0.03

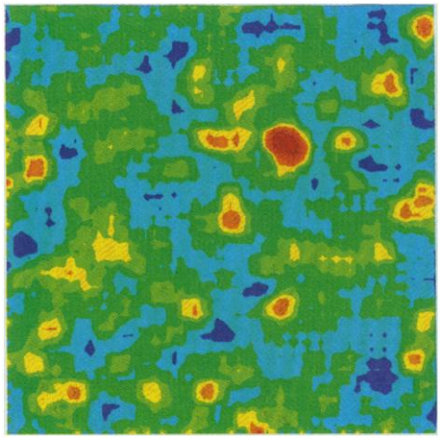

Fig. 1. The density field of a three-dimensional box of a CHDM simulation projected onto a plane as a translucent rendering of the volume. Red corresponds to high-density peaks and blue to low-density regions in a rainbowlike sequence. Different structures dominate at different length scales, illustrating the underlying multifractal structure that produces the empirically observed multiscaling.

Multiscaling behavior is clearly present in these simulations: D_2 varies with the characteristic interparticle distance of each sample d_i. We have also analyzed the variation of the correlation length r_0 as a function of d_i calculated by means of Eq. 4. Results are given in Table 1 and correspond to fitting $C(r)$ over the scale range $10h^{-1}$ to $50h^{-1}$ Mpc. As expected on the basis of our multiscaling hypothesis, richer clusters (that is, with larger d_i) generate less steep $C(r)$ and larger r_0. The remarkably small errors in the fitting parameters (especially on D_2) show that there is an excellent power-law fit to $C(r)$ over the entire range of scales considered.

A similar qualitative behavior is manifested by the observed distribution of cosmic objects. If galaxies and galaxy systems with increasing richness are considered to be selected by applying a density threshold in the mass distribution, the multiscaling argument implies that the corresponding values of the correlation dimension D_2 must decrease with increasing density. We show here the results of a correlation integral analysis of different galaxy and cluster samples. For galaxies we use the Center for Astrophysics (CfA) sample (*2*), the Perseus-Pisces sample (*24*), and the QDOT (Queen Mary, Durham, Oxford, and Toronto)-IRAS redshift survey (*25*). The cluster samples used are the Abell and ACO (Abell-Corwin-Olowin) catalogs (*26*), the Edinburgh-Durham Cluster Catalog (EDCC) redshift survey (*8*), the ROSAT x-ray–selected cluster sample (*10*), and the APM (Automated Plate Measuring) cluster catalog (*9*). We have performed the calculation of $C(r)$ directly on the CfA and QDOT galaxy surveys and Abell and ACO catalogs; in the other cases we just have integrated the published values of $\xi(r)$. Although this latter procedure is straightforward, the numerical integration does tend to exaggerate errors: direct calculations of $C(r)$ are generally better.

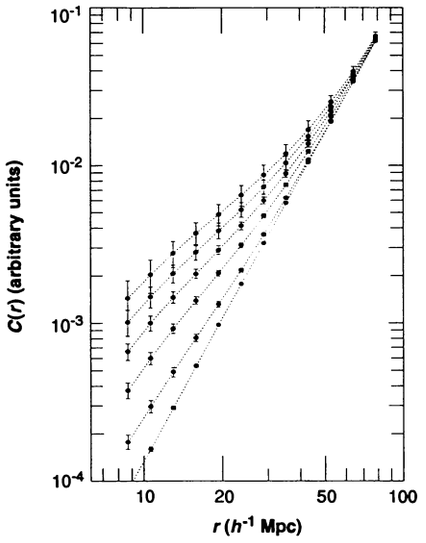

Fig. 2. The correlation integral $C(r)$ for the cluster samples drawn from CHDM simulations in a cubic volume of side $320h^{-1}$ Mpc. We plot averages over 50 realizations of this model; error bars correspond to the 1σ scatter evaluated over the ensemble. Arbitrary units are chosen for $C(r)$ to make all of the curves coincident at large separations. Going from top to bottom, we plot results for progressively lower values of the mean separation d_i.

The x-ray, Abell, ACO, and APM cluster correlation integrals are all well-fit by a power law with exponent $D_2 \approx 2.1$ (Fig. 3). The EDCC sample yields a value of $D_2 \approx 1.8$ over the same scaling range. A value of $D_2 \approx 2.5$ applies to the optical galaxy catalogs (CfA and Perseus-Pisces), and a value of $D_2 \approx 2.8$ is obtained for the QDOT-IRAS galaxies. These values for D_2 are quite different from those obtained with $\gamma \approx 1.8$ for the slope of $\xi(r)$ and in the relation $D_2 = 3 - \gamma$. This is essentially because the range of scales for which we obtain the various estimates of D_2 in Fig. 2 does not coincide with the range where $\xi_{gg}(r)$ behaves as a power law; clusters of galaxies sample this range of scales particu-

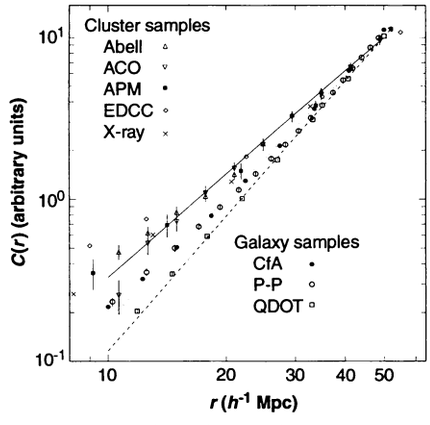

Fig. 3. The correlation integral $C(r)$ for the galaxy and cluster samples. The distribution of most of the cluster samples are well described by a power law with an exponent $D_2 = 2.1$ (solid line), although the EDCC samples are better described by $D_2 = 1.8$. The CfA and Perseus-Pisces (P-P) galaxy samples (dotted line) have $D_2 = 2.5$, and the QDOT-IRAS galaxies (dashed line) have $D_2 = 2.8$. Results are given in arbitrary units because $C(r)$ has been rescaled to facilitate comparison of the different slopes D_2. Bootstrap errors are plotted for several samples.

larly poorly. Because the smaller D_2 is, the larger is the departure from a uniform space-filling distribution, these results mean that clusters of galaxies have stronger correlations than optical galaxies, which, in turn, have stronger correlations than IRAS galaxies. It is natural to interpret these trends in terms of multiscaling of objects identified in terms of different richness thresholds. A self-consistent picture emerges in which clusters correspond to higher matter densities than typical optical galaxies, which are themselves located (on average) in denser environments than IRAS galaxies. Even the apparently anomalous behavior of EDCC is consistent with this trend: clusters from this sample are, on average, richer than in the other cluster samples, so its behavior confirms the multiscaling of clusters of different density seen in the simulations we have already described.

An important point to emerge from this analysis is that the most natural and effective way to characterize scaling properties of the clustering of objects of different intrinsic richness is through the correlation integral $C(r)$ rather than the two-point correlation function $\xi(r)$. Although differences in the two descriptions are small if $\xi(r) \gg 1$, in the regime where $\xi \approx 1$, no distribution can simultaneously display scaling of both $\xi(r)$ and $C(r)$. The correlation integral description allows a wide range of empirical clustering data to be unified into a single coherent framework within which multiscaling is a natural consequence. For example, the fact that D_2 for IRAS galaxies is larger than that for optical samples indicates that IRAS galaxies are less correlated than optical galaxies, or in other words, that optical galaxies correspond to higher peaks of the density distribution.

Using Eq. 4, we can obtain clean estimates of r_0 for these data sets. For the ACO sample, we get $r_0 \approx 23h^{-1}$ Mpc, and for the Abell sample, $r_0 \approx 26h^{-1}$ Mpc in the range $10h^{-1}$ to $50h^{-1}$ Mpc, whereas for the APM cluster catalog, we get $r_0 \approx 16.7h^{-1}$ Mpc in the range $1h^{-1}$ to $40h^{-1}$ Mpc, in agreement with the value reported by Dalton *et al.* fitting $\xi(r)$ directly to a power law (9).

What is missing at the moment from this approach is a detailed understanding of the way initial conditions and dynamics interact to produce the observed scaling properties. Nevertheless, the ability to incorporate the dependence of clustering strength on richness into a unified multifractal scaling paradigm through the multiscaling hypothesis is a considerable benefit of this approach. Moreover, the robustness of $C(r)$ scaling compared to that of $\xi(r)$ strongly motivates the use of $C(r)$ as a diagnostic of clustering pattern and dynamics. Only by the use of appropriate statistical tools such as this will the new generation of galaxy redshift surveys lead to a theoretical understanding of the origin of large-scale structure in the universe.

REFERENCES AND NOTES

1. M. Davis, A. Meiksin, M. A. Strauss, L. N. da Costa, A. Yahil, *Astrophys. J.* **333**, L9 (1988).
2. V. J. Martínez, M. Portilla, B. J. T. Jones, S. Paredes, *Astron. Astrophys.* **280**, 5 (1993).
3. M. Postman, M. J. Geller, J. P. Huchra, *Astrophys. J.* **384**, 404 (1992).
4. W. Sutherland and G. Efstathiou, *Mon. Not. R. Astron. Soc.* **248**, 159 (1991).
5. Y. P. Jing, M. Plionis, R. Valdarnini, *Astrophys. J.* **389**, 499 (1992).
6. G. Efstathiou, G. B. Dalton, W. J. Sutherland, S. J. Maddox, *Mon. Not. R. Astron. Soc.* **257**, 125 (1992).
7. N. A. Bahcall, R. M. Soneira, W. S. Burgett, *Astrophys. J.* **311**, 15 (1986).
8. R. C. Nichol, C. A. Collins, L. Guzzo, S. L. Lumsden, *Mon. Not. R. Astron. Soc.* **255**, 21P (1992).
9. G. B. Dalton *et al.*, *ibid.* **271**, L47 (1994).
10. A. K. Romer *et al.*, *Nature* **372**, 75 (1994).
11. J. A. Peacock and M. J. West, *Mon. Not. R. Astron. Soc.* **259**, 494 (1992).
12. M. Plionis and S. Borgani, *ibid.* **254**, 306 (1992).
13. A. S. Szalay and D. N. Schramm, *Nature* **314**, 718 (1985).
14. N. A. Bahcall and M. J. West, *Astrophys. J.* **392**, 419 (1992).
15. X. Luo and D. N. Schramm, *Science* **256**, 513 (1992).
16. R. A. Croft and G. Efstathiou, *Mon. Not. R. Astron. Soc.* **267**, 390 (1994).
17. S. Borgani, M. Plionis, P. Coles, L. Moscardini, *ibid.*, in press.
18. P. J. E. Peebles, *Physical Cosmology* (Princeton, NJ, 1993).
19. G. Paladin and A. Vulpiani, *Phys. Rep.* **156**, 147 (1987).
20. S. Borgani, *ibid.* **251**, 1 (1995); B. J. T. Jones, V. J. Martínez, E. Saar, J. Einasto, *Astrophys. J.* **332**, L1 (1988); V. J. Martínez, B. J. T. Jones, R. Dominguez-Tenreiro, R. Van de Weygaert, *ibid.* **357**, 90 (1990); B. J. T. Jones, P. Coles, V. J. Martínez, *Mon. Not. R. Astron. Soc.* **259**, 146 (1992); R. Valdarnini, S. Borgani, A. Provenzale, *Astrophys. J.* **394**, 422 (1992).
21. M. H. Jensen, G. Paladin, A. Vulpiani, *Phys. Rev. Lett.* **67**, 208 (1991); G. Paladin, M. Vergassola, A. Vulpiani, *Physica A* **185**, 174 (1992).
22. N. Kaiser, *Astrophys. J.* **284**, L9 (1984); J. M. Bardeen, J. R. Bond, N. Kaiser, A. S. Szalay, *ibid.* **304**, 15 (1986).
23. A. Klypin, J. Holtzman, J. Primack, E. Regös, *ibid.* **416**, 1 (1993).
24. L. Guzzo, A. Iovino, G. Chincarini, R. Giovanelli, M. P. Haynes, *ibid.* **382**, L5 (1992).
25. V. J. Martínez and P. Coles, *ibid.* **437**, 550 (1994).
26. S. Borgani, V. J. Martínez, M. A. Pérez, R. Valdarnini, *ibid.* **435**, 37 (1994).

27. We thank L. Guzzo, K. Romer, and G. Dalton for making their $\xi(r)$ results available to us. We are also grateful to L. Moscardini and M. Plionis for permission to use cluster simulations done by them together with P.C. and S.B. The Particle Physics and Astronomy Research Council provides P.C. with an Advanced Research Fellowship. S.P. is supported by a fellowship of the Ministerio de Educación y Ciencia. This research was partially supported by a European Community Human Capital and Mobility Programme network (contract ERB CHRX-CT93-0129) and by the project GV-2207/94 of the Generalitat Valenciana.

13 April 1995; accepted 13 July 1995

Biological Controls on Coral Sr/Ca and $\delta^{18}O$ Reconstructions of Sea Surface Temperatures

Stephanie de Villiers,* Bruce K. Nelson, Allan R. Chivas

Coral strontium/calcium ratios have been used to infer that the tropical sea surface temperature (SST) cooled by as much as 6°C during the last glacial maximum. In contrast, little or no change has been inferred from other marine-based proxy records. Experimental studies of the effect of growth rate and the magnitude of intraspecific differences indicate that biological controls on coral skeletal strontium/calcium uptake have been underestimated. These results call into question the reliability of strontium/calcium–based SST reconstructions.

Paleoclimate reconstructions of tropical SSTs during the last glacial maximum (LGM) have produced contradictory results: Continental temperature proxy records suggest that the tropics were 4° to 6°C colder during the LGM (*1*), as opposed to estimates from planktonic microfossil assemblages, which suggest little or no change (*2*). The resolution of this discrepancy is key to establishing the sensitivity of the tropics to global climate change (*3*). The Sr/Ca content of coral skeletons has recently been used as a proxy for SST (*4*, *5*). The basic principle is that the correlative relation between coral Sr/Ca and SST can be applied to fossil coral specimens to reconstruct SSTs in paleoenvironments. The Sr/Ca measurement precision of <0.1%, equivalent to ~0.1°C, is 10 times that of other paleothermometers (*4*). The Sr/Ca results suggest that the tropical western Pacific and western Atlantic were 4° to 6°C cooler during the LGM than today (*4*, *5*); this estimate is in agreement with terrestrial temperature proxy records but contradicts other marine-based records (*1*–*3*).

Two key assumptions are made in apply-

S. de Villiers, School of Oceanography, University of Washington, Box 357940, Seattle, WA 98195–7940, USA.
B. K. Nelson, Department of Geological Sciences, University of Washington, Seattle, WA 98195, USA.
A. R. Chivas, Research School of Earth Sciences, Australian National University, Canberra ACT 0200, Australia.
*To whom correspondence should be addressed. Present address: Sea Fisheries Research Institute, Department of Environment Affairs, Private Bag X2, Cape Town 8012, South Africa.